JACS
JOURNAL OF THE AMERICAN CHEMICAL SOCIETY
Article
pubs.acs.org/JACS

A Cyclic Peptide Inhibitor of HIF-1 Heterodimerization That Inhibits Hypoxia Signaling in Cancer Cells

Elena Miranda,[†,#] Ida K. Nordgren,[†,#] Abigail L. Male,[†] Charlotte E. Lawrence,[†] Franciane Hoakwie,[†] Francesco Cuda,[†] William Court,[∥] Keith R. Fox,[‡,§] Paul A. Townsend,[§,⊥,▽] Graham K. Packham,[§,⊥] Suzanne A. Eccles,[∥] and Ali Tavassoli*[,†,§,⊥]

[†]Chemistry, [‡]Centre for Biological Sciences, [§]Institute for Life Sciences, University of Southampton, Southampton SO17 1BJ, United Kingdom

[∥]Cancer Research UK Cancer Therapeutics Unit, The Institute of Cancer Research, Sutton SM2 5NG, United Kingdom

[⊥]Cancer Sciences, Faculty of Medicine, University of Southampton, Southampton SO16 6YD, United Kingdom

Supporting Information

ABSTRACT: Hypoxia inducible factor-1 (HIF-1) is a heterodimeric transcription factor that acts as the master regulator of cellular response to reduced oxygen levels, thus playing a key role in the adaptation, survival, and progression of tumors. Here we report *cyclo*-CLLFVY, identified from a library of 3.2 million cyclic hexapeptides using a genetically encoded high-throughput screening platform, as an inhibitor of the HIF-1α/HIF-1β protein−protein interaction in vitro and in cells. The identified compound inhibits HIF-1 dimerization and transcription activity by binding to the PAS-B domain of HIF-1α, reducing HIF-1-mediated hypoxia response signaling in a variety of cell lines, without affecting the function of the closely related HIF-2 isoform. The reported cyclic peptide demonstrates the utility of our high-throughput screening platform for the identification of protein−protein interaction inhibitors, and forms the starting point for the development of HIF-1 targeted cancer therapeutics.

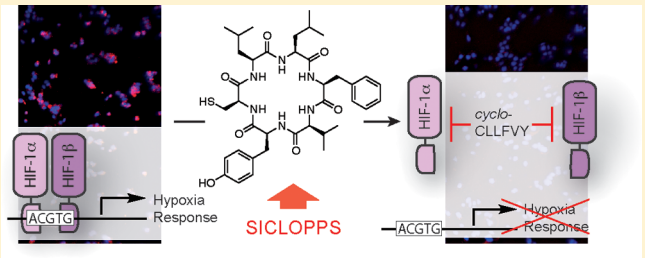

INTRODUCTION

Homeostasis of oxygen, a key metabolite, is critical for mammalian cell survival. This necessitates a robust network that senses and rapidly responds to hypoxia (low oxygen levels). The key component of this hypoxia response network is hypoxia-inducible factor (HIF), a heterodimeric transcription factor composed of an oxygen-regulated α-subunit and a ubiquitously expressed β-subunit (also known as the aryl nuclear transcription factor or ARNT). Mammals possess three isoforms of HIF-α; the ubiquitously expressed HIF-1α mounts the immediate response to reductions in cellular oxygen,[1] while HIF-2α (also known as EPAS1) and HIF-3α are thought to regulate the response to prolonged hypoxia. While the intricate interplay between HIF-α isoforms in cancer is complicated and yet to be fully deciphered,[2] the role of HIF-1 activity in angiogenesis, tumor growth, and metastasis is well established.[3,4] HIF-1α is overexpressed in many cancers,[5] and oncogene activation and loss of tumor suppressor function is shown to be associated with HIF-1 activation.[6]

HIF-1α is negatively regulated at the protein level by oxygen via prolyl hydroxylase enzymes that use oxygen as a substrate for the hydroxylation of residues 402 and 564 of HIF-1α, marking it for ubiquitination by an E3 ubiquitin ligase complex and rapid proteolysis.[7,8] Reduced oxygen levels lead to the stabilization and nuclear translocation of HIF-1α,[9] where it binds HIF-1β to form the HIF-1 transcription factor complex. HIF-1 rapidly mounts a transcriptional response to hypoxia[1,10] by directing the expression of a wide variety of hypoxia response genes.[11,12] By utilizing changes in the substrate concentration of a continuously occurring enzymatic reaction (hydroxylation of HIF-1α), the cellular response to hypoxia is near instantaneous,[13] with HIF-1α acting as both the sensor and a key component of the hypoxia response machinery.

Inhibition of HIF-1 has long been known to hold much potential for cancer therapy;[14] there are multiple possible points for therapeutic intervention in the hypoxia response network, and molecules that inhibit various components of this diverse pathway have been reported,[15−22] but the absolute requirement for the dimerization of HIF-1α and HIF-1β for DNA binding and transcription activity of the HIF-1 complex makes this protein−protein interaction a seemingly optimal point of interception. Several high-throughput screens have been conducted in the effort to identify HIF-1 inhibitors,[15,19,21,22] but there are currently no selective inhibitors of the HIF-1α/HIF-1β protein−protein interaction. The only reported inhibitor of HIF-1 dimerization is the heteroaromatic

Received: March 25, 2013
Published: June 24, 2013

   dx.doi.org/10.1021/ja402993u | J. Am. Chem. Soc. 2013, 135, 10418−10425

acridine derivative acriflavine, which nonselectively inhibits both HIF-1 and HIF-2.[19]

A compound that specifically inhibits HIF-1 dimerization in cells will not only serve as a chemical tool to decipher the mechanism of hypoxia response, but would also form the starting point for the development of HIF-1-directed therapeutic agents. Here we report an inhibitor of the HIF-1α/HIF-1β protein−protein interaction, identified from a genetically encoded library of 3.2 million cyclic peptides. The most potent identified cyclic peptide (*cyclo*-CLLFVY) inhibits HIF-1 dimerization in vitro and in cells by binding to the PAS-B domain of HIF-1α, and prevents HIF-1- but not HIF-2-mediated hypoxia signaling in a variety of cell lines.

RESULTS AND DISCUSSION

Identification of HIF-1 Heterodimerization Inhibitors Using a Genetically Encoded High-Throughput Screening Platform. We used our genetically encoded high-throughput screening platform[23−25] to identify inhibitors of the HIF-1α/HIF-1β protein−protein interaction. We built and verified the function of a HIF-1 bacterial reverse two-hybrid system (RTHS, for a detailed description see the Supporting Information and Figures S1−S3). The HIF-1 RTHS was used to screen a plasmid-encoded SICLOPPS (split intein circular ligation of peptides and proteins)[26,27] library of 3.2 million cyclic hexapeptides for HIF-1 dimerization inhibitors.

After the first round of screening, 120 surviving colonies were observed and subjected to several rounds of secondary screening to eliminate false positives and nonselective inhibitors, leaving 12 potential HIF-1 dimerization inhibitors that were ranked by drop-spotting. Four of these peptides were significantly more active than the others; the SICLOPPS plasmids encoding these 4 peptides were sequenced to reveal the identity of the HIF-1 inhibitors as *cyclo*-CLLFVY (encoded by two SICLOPPS plasmids), *cyclo*-CRLMVL, and *cyclo*-CLLRMY (Figure 1, *R* = H). Interestingly, the two isolated

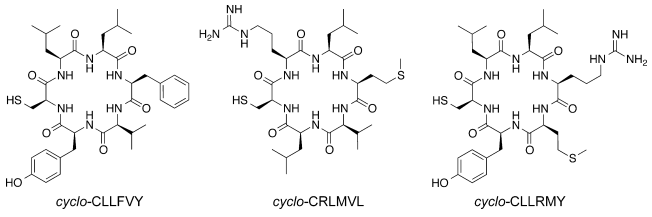

Figure 1. Cyclic peptide HIF-1 inhibitors. Cyclic peptide HIF-1 inhibitors identified from a SICLOPPS library of 3.2 million cyclic hexapeptides (R = H).

cyclo-CLLFVY plasmids encoded the peptide via different codons. To ensure that the cyclic peptides, not their unspliced peptide aptamers, were responsible for the observed inhibition of HIF-1, we utilized mutant SICLOPPS dnaE C-terminal inteins (H24A, F26A) that do not splice.[28] The unspliced peptides lost the ability of their parent cyclic equivalents to disrupt HIF-1α/HIF-1β dimerization (Figure S3B), demonstrating that HIF-1 inhibition by these peptides is dependent on their cyclic form.

The three identified HIF-1 inhibitors were synthesized and tagged with Tat peptide (via a disulfide bond between the set cysteine of the cyclic peptide and a cysteine introduced to the start of Tat)[25] to aid the translocation across the plasma membrane of mammalian cells. In the following experiments, Tat-*cyclo*-CLLFVY is referred to as P1, Tat-*cyclo*-CRLMVL as P2, and Tat-*cyclo*-CLLRMY as P3 (Figure 1, R = CGRKKRRQRRRPPQ).

P1 Inhibits HIF-1 Activity in a Mammalian Cell Luciferase Reporter Assay. The ability of P1−P3 to disrupt HIF-1 function in cells was assessed using a HIF-1-dependent luciferase reporter assay.[15,21] The assay uses human osteosarcoma U2OS cells, stably transfected with a HIF-dependent luciferase reporter construct (U2OS-HRE-luc), where activation of HIF results in an increase in luciferase expression.[15]

Hypoxia (1% O_2) results in a ∼12-fold increase in the luciferase signal, which is inhibited in a dose-dependent manner by P1 (IC_{50} of 19 ± 2 μM); P1 did not alter basal luciferase activity in normoxia (Figure 2A). P2 and P3 did not show an effect on the luciferase reporter in hypoxia or normoxia. P1−P3

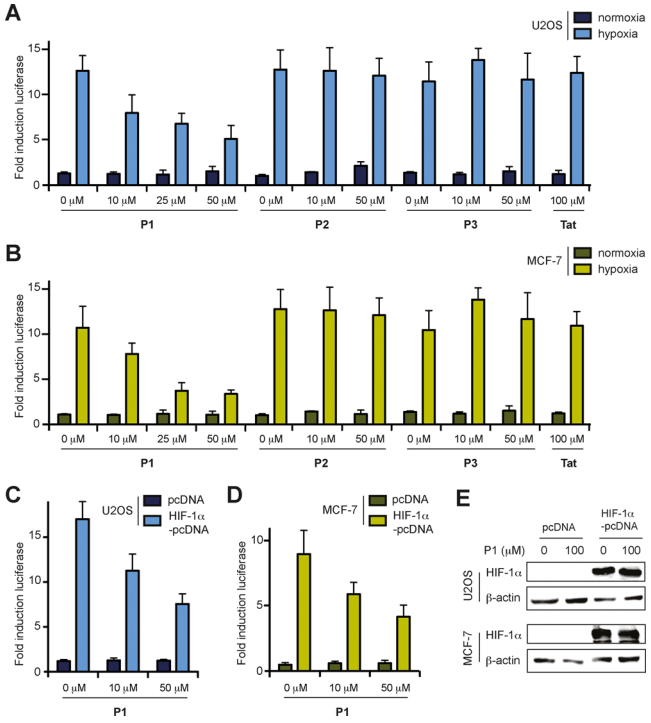

Figure 2. Effect of P1−P3 in a HIF-1 luciferase-reporter assay. Data shows fold-increase of the luciferase signal compared to untreated cells in normoxia. (A) P1 causes a dose-dependent reduction in the HIF-1-mediated luciferase signal in hypoxic U2OS cells. (B) Assay in (A) repeated in MCF-7 cells. (C) P1 inhibits the HIF-1-mediated luciferase signal in a normoxic reporter assay in U2OS cells. (D) Assay in (C) repeated in MCF-7 cells. (E) Representative blots showing that 100 μM P1 does not alter HIF-1α protein levels in the cells in (C) and (D).

had no effect in the U2OS-luc control cell line[15] stably expressing luciferase (Figure S4), indicating that P1 does not inhibit endogenous cellular processes such as transcription or translation. To assess the cell-specificity of P1, the experiment was repeated in MCF-7 breast cancer cells with similar results (P1 IC_{50} of 16 ± 1 μM) (Figure 2B). Tat-tag alone (100 μM) did not affect the luciferase signal in these assays (Figure 2A and 2B).

HIF-1 has been shown to directly promote the expression of HIF-1α in hypoxia by binding to a hypoxia-response element (HRE) upstream of the HIF-1α.[29] This has been shown to be dependent on the methylation state of a cytosine in the HIF-1 binding site (ACGTG) upstream of HIF-1α; a methylated

dx.doi.org/10.1021/ja402993u | J. Am. Chem. Soc. 2013, 135, 10418−10425

cytosine prevents HIF-1 binding and inhibits the autotransactivation of HIF-1α in hypoxia.[29] Bisulfite sequencing of this region of MCF-7 and U2OS cells revealed this HRE to be unmethylated, and thus, an inhibitor of HIF-1α/HIF-1β dimerization would potentially reduce the HIF-1-promoted upregulation of HIF-1α mRNA and protein levels in these cell lines. The reduction of luciferase signal observed in P1-treated U2OS and MCF-7 cells (Figure 2A and B) could therefore be partially a result of a reduction in hypoxic HIF-1α levels (this would be the case for any inhibitor of HIF-1 dimerization in these cell lines). To decouple P1's effect on HIF-1α transactivation from its effect on HIF-1α/HIF-1β dimerization, a normoxic luciferase-reporter assay was devised where HIF-1α is expressed from a transiently transfected vector, resulting in continuously elevated levels of HIF-1α in normoxic cells. P1 continued to inhibit the luciferase signal in both U2OS and MCF-7 cells in this assay (Figure 2C and D), with HIF-1α protein levels not being altered by P1 (Figure 2E).

The observed discrepancy between the activity of *cyclo*-CRLMVL and *cyclo*-CLLRMY in the HIF-1 RTHS (Figure S3B), and the lack of activity of P2 and P3 in the luciferase assay (Figure 2) is likely due to the ±10-fold range in each step of the drop-spotting assay; P2 and P3 may be up to 10-fold less active than P1 and still result in the same drop-spotting pattern. P1 was therefore taken forward for further assessment of its activity. P2, a Tat-tagged cyclic hexapeptide that differs from P1 by two amino acids, was used as a negative control in the following experiments.

***cyclo*-CLLFVY Disrupts HIF-1, but Not HIF-2 Dimerization in vitro by Binding to the PAS-B Domain of HIF-1α.** We next probed the effect of *cyclo*-CLLFVY on the interaction of HIF-1α with HIF-1β in vitro. Recombinant His-HIF-1α_{1-350} and GST-HIF-1β_{1-474} were produced and purified. Electrophoretic mobility shift assay (EMSA) was used to demonstrate that the recombinant HIF-1 proteins form functional heterodimers (Figure S5A). Unfortunately, the positively charged Tat-tag of P1 is incompatible with EMSA (interferes with the bandshift of DNA). We therefore assessed the ability of P1 to disrupt HIF-1 dimerization by enzyme-linked immunosorbent assay (ELISA); P1 was found to disrupt the protein−protein interaction of His-HIF-1α_{1-350} and GST-HIF-1β_{1-474} with an IC_{50} of 1.3 μM (Figure 3A). The control compound P2 had no effect on HIF-1 dimerization in this assay (Figure S6). To determine the HIF-1-specificity of *cyclo*-CLLFVY, we assessed its ability to disrupt HIF-2 dimerization by ELISA. Recombinant His-HIF-2α_{1-351} was produced and purified, and shown to form functional heterodimers with GST-HIF-1β_{1-474} by EMSA (Figure S5B). P1 had no effect on the dimerization of His-HIF-2α_{1-351} with GST-HIF-1β_{1-474} (Figure 3B).

To identify the target (HIF-1α or HIF-1β) of our HIF-1 inhibitor, we synthesized a biotinylated derivative of *cyclo*-CLLFVY for use as bait in pull-down assays by replacing the cysteine residue (present in all members of the SICLOPPS library to allow intein splicing) with propargylalanine. This compound was linked to biotin-PEG-azide by click-chemistry (copper-catalyzed alkyne azide reaction) to give biotin-PEG-triazole-*cyclo*-ALLFVY as the bait molecule. The bait was immobilized onto streptavidin-coated beads and mixed with recombinant His-HIF-1α_{1-350} and GST-HIF-1β_{1-474}. The pulled-down protein(s) were analyzed by Western blot, revealing His-HIF-1α_{1-350} as the target of *cyclo*-CLLFVY (Figure 3C, lane 3). Streptavidin beads did not pull down either HIF-1 subunit in the absence of the bait molecule (Figure 3C, lane 2), and propargylalanine click-linked to biotin-PEG-azide did not pull

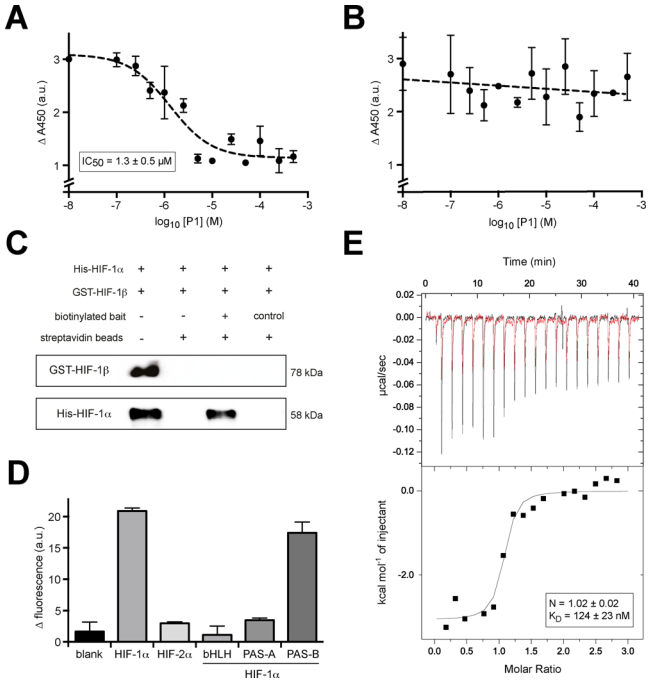

Figure 3. Assessing the activity of *cyclo*-CLLFVY in vitro. (A) Effect of 10 nM to 500 μM P1 on the heterodimerization of His-HIF-1α_{1-350} with GST-HIF-1β_{1-474} analyzed by ELISA; P1 disrupts this interaction with an IC_{50} of 1.3 ± 0.5 μM. (B) Effect of 10 nM to 500 μM P1 on the interaction of His-HIF-2α_{1-351} with GST-HIF-1β_{1-474}; P1 does not affect HIF-2 heterodimerization. (C) His-HIF-1α_{1-350} is selectively pulled-down by streptavidin beads coated with biotin-PEG-triazole-*cyclo*-ALLFVY (lane 3); lane 1 is the loading control. Neither protein is pulled-down by streptavidin beads alone (lane 2), or streptavidin beads coated with a biotin-linked control (lane 4). (D) Fluorescent binding assay showing a Megastoke 673-labeled derivative of *cyclo*-CLLFVY binding to His-HIF-1α_{1-350}, while its binding to His-HIF-2α_{1-351} is close to background levels. The fluorescent derivative of *cyclo*-CLLFVY binds the PAS-B domain of HIF-1α, whereas binding to bHLH and PAS-A domains are close to background level. (E) ITC shows P1 binding to the PAS-B domain of HIF-1α with 1:1 stoichiometry and 124 ± 23 nM affinity. Red line shows control P1 injection into buffer only.

down either HIF-1 subunit (Figure 3C, lane 4). To verify binding of *cyclo*-CLLFVY to HIF-1α, we used the propargylalanine derivative of this molecule and azide-Megastoke dye 673 to synthesize a fluorescent derivative by click-chemistry. His-HIF-1α_{1-350} and His-HIF-2α_{1-351} were immobilized onto Ni^{2+}-coated 96-well plates, and the fluorescent analogue of *cyclo*-CLLFVY was washed over these proteins. Binding of the fluorescent derivative to these proteins was monitored via increased fluorescence at 680 nm. We observed binding of the fluorescent derivative of *cyclo*-CLLFVY to His-HIF-1α_{1-350}, with binding to His-HIF-2α_{1-351} at close to background levels (Figure 3D).

We next sought to identify the domain of HIF-1α bound by *cyclo*-CLLFVY. The HIF-1α protein used in our RTHS is composed of the DNA-binding basic-helix−loop−helix domain (bHLH, amino acids 1−80) and the protein−protein interaction Per-ARNT-SIM-A (PAS-A, amino acids 90−155) and Per-ARNT-Sim-B (PAS-B, amino acids 235−350) domains. Recombinant His-bHLH, His-PAS-A, and His-PAS-B domains were immobilized onto Ni^{2+}-coated 96-well plates, and the fluorescent derivative of *cyclo*-CLLFVY was washed over the bound proteins. We observed an increase in fluorescence (at 680 nm) of the PAS-B domain,

dx.doi.org/10.1021/ja402993u | J. Am. Chem. Soc. 2013, 135, 10418−10425

whereas bHLH and PAS-A remained close to background, indicating binding of our inhibitor to the PAS-B domain of HIF-1α (Figure 3D). We next used P1 in isothermal titration calorimetry (ITC) to verify these observations and quantify binding affinities; P1 bound the PAS-B domain of HIF-1α in 1:1 stoichiometry and with a K_D of 124 nM (Figure 3E). P1 did not bind to the bHLH or PAS-A domain of HIF-1α (Figures S7A and B), and P2 did not bind the HIF-1α PAS-B domain (Figure S7C). P1 did not bind HIF-1β_{1-474} (Figure S7D). The observed selectivity of P1 for HIF-1 over HIF-2 in vitro (Figure 3A versus B, and 3D) suggests the possibility of selectivity for HIF-1 over HIF-2 in cells.

P1 Disrupts HIF-1 Dimerization in MCF-7 and U2OS Cells. The effect of P1 on the endogenous HIF-1α/HIF-1β interaction in intact cells was directly probed using an in situ proximity ligation assay (PLA);[30] primary antibodies (HIF-1α and HIF-1β here) raised in different species are bound by specific secondary antibodies that are tagged with a short DNA strand. The DNA on the interacting PLA probes forms a mini-plasmid that is amplified and bound by a red fluorescent dye. The HIF-1α/HIF-1β interaction is thus visualized as red dots in the DAPI-stained nuclei of MCF-7 and U2OS cells (Figure 4).

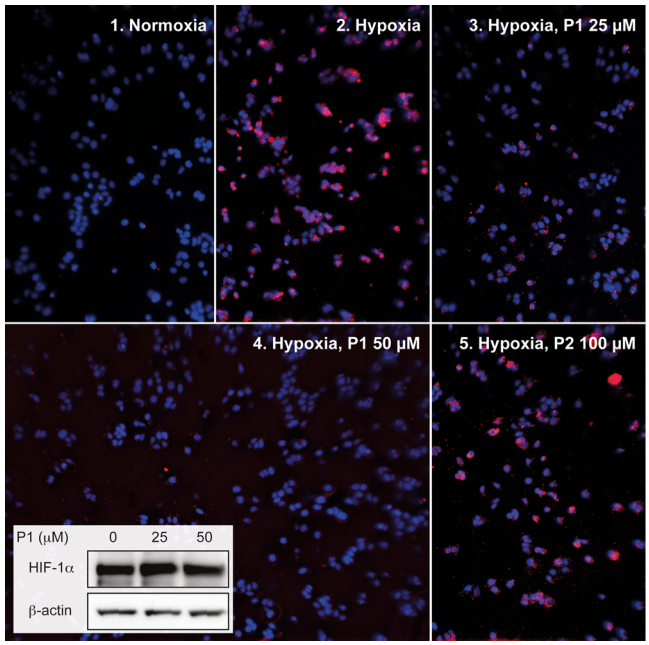

Figure 4. Inhibition of HIF-1 dimerization by *cyclo*-CLLFVY assessed by immunofluorescence detection of endogenous HIF-1α/HIF-1β dimerization by in situ PLA in MCF-7 cells. The PLA signal is absent in normoxia (panel 1) but readily observed in hypoxia (panel 2). P1-treatment (25 or 50 μM) of hypoxic cells results in a loss of the PLA signal (panels 3 and 4, respectively), whereas 100 μM P2 shows no effect (panel 5). Inset: Western blot analysis of cell lysates show that P1 does not affect HIF-1α levels in this assay.

We observed an increase in PLA signal in MCF-7 cells incubated in hypoxia (1% O_2) for 4 h, indicating the expected formation of the HIF-1 dimer in hypoxia (Figure 4, panel 1 versus panel 2). Hypoxic MCF-7 cells dosed with 25 and 50 μM P1 showed a reduction in the HIF-1 PLA signal (Figure 4, panels 3 and 4). P2 at 100 μM did not have any effect on the PLA signal (Figure 4, panel 5). The observed effect is not due to a reduction in HIF-1α by P1 (Western blot inset in Figure 4) and thus may be solely attributed to disruption of HIF-1α/HIF-1β dimers.

P1 Inhibits HIF-1-Mediated Cellular Hypoxia Response. The effect of P1's disruption of the HIF-1α/HIF-1β heterodimer on cellular hypoxia response was next characterized. We measured the effect of P1 on vascular endothelial growth factor (VEGF), a HIF-1 regulated gene that stimulates vasculogenesis and angiogenesis in hypoxia.[31] The transcription of VEGF increased ~3-fold after incubation for 16 h in hypoxia in untreated MCF-7 and U2OS cells; P1-treated cells showed a dose-dependent reduction in VEGF mRNA in both cell lines, while the control peptide P2 (100 μM) had no effect (Figure 5A). VEGF protein levels increased 3- to 5-fold in both MCF-7 and U2OS cells after 16 h of incubation in hypoxia, with P1-treatment resulting in a dose-dependent reduction of VEGF protein (measured by a quantitative immunoassay) in both cell lines; pretreatment with 50 μM of P1 fully inhibited the hypoxic induction of VEGF protein, resulting in normoxic VEGF levels in hypoxic MCF-7 and U2OS cells (Figures 5B). As VEGF is a regulator of angiogenesis, we next probed the effect of P1 on HIF-1 mediated tubule formation in hypoxic human umbilical vein endothelial cells (HUVEC),[32] and observed a dose-dependent reduction of HUVEC tubularization in P1-treated cells, with no effect from P2 (Figure 5C; for representative images, see Figure S8). The effect of P1 on HIF-1 signaling was further assessed via carbonic anhydrase IX (CAIX), an extracellular metalloenzyme whose expression is significantly upregulated (~25-fold) by HIF-1 after 16 h incubation in hypoxia.[33] Treatment of MCF-7 and U2OS cells with 50 μM P1 resulted in a 5-fold reduction of CAIX mRNA in hypoxia, with no effect from 100 μM P2 (Figure 5D). A sulforhodamine B (SRB) cytotoxicity assay[34] was used to demonstrate that the observed effects are not due to toxicity of P1 (Figure 5E). The cytotoxicity and effect of P1 on cell proliferation was further probed by measuring the effect of increasing doses of P1 (1−100 μM) on MCF-7 cells over 72 h, with 1 μM 4-hydroxytamoxifen used as a positive control. P1 at 100 μM did not affect the viability of MCF-7 cells, whereas 1 μM 4-hydroxytamoxifen inhibited proliferation as expected (Figure 5F).

P1 Does Not Affect HIF-2-Mediated Hypoxia Signaling. The cellular HIF-1-specificity of P1 was probed using 786-O cells, a VHL-defective renal cell carcinomal line that does not express detectable levels of HIF-1α, but instead expresses HIF-2α at a high constitutive level.[35] This results in regulation of hypoxia response genes such as VEGF and lysyl oxidase (LOX) in 786-O cells by HIF-2 instead of HIF-1.[36] We reasoned that if P1 also inhibits the dimerization of HIF-2 in cells, a dose-dependent reduction in the mRNA and protein products of these hypoxia response genes would be observed in hypoxic 786-O cells, whereas a specific HIF-1 inhibitor would not affect hypoxia-response in this cell line. In contrast to MCF-7 and U2OS cells, P1 at concentrations up to 100 μM had no effect on a variety of HIF-2-promoted genes in 786-O cells (Figure 6A). In addition, P1 had no effect on VEGF protein levels in hypoxic 786-O cells (Figure 6B). To further probe the effect of P1 on HIF-2, a luciferase reporter assay was developed and used. The assay was derived from the HIF-1 luciferase reporter assay detailed above (Figure 2C and D) and adapted for HIF-2 by replacing the plasmid encoding HIF-1α with the equivalent plasmid encoding HIF-2α. P1 did not affect the luciferase reporter signal in MCF-7 or U2OS cells (Figure 6C and D), providing additional evidence that P1 inhibits HIF-1, but not HIF-2 signaling in cells. P2 and P3 also had no effect on HIF-2 in this assay (Figure S9).

dx.doi.org/10.1021/ja402993u | J. Am. Chem. Soc. 2013, 135, 10418−10425

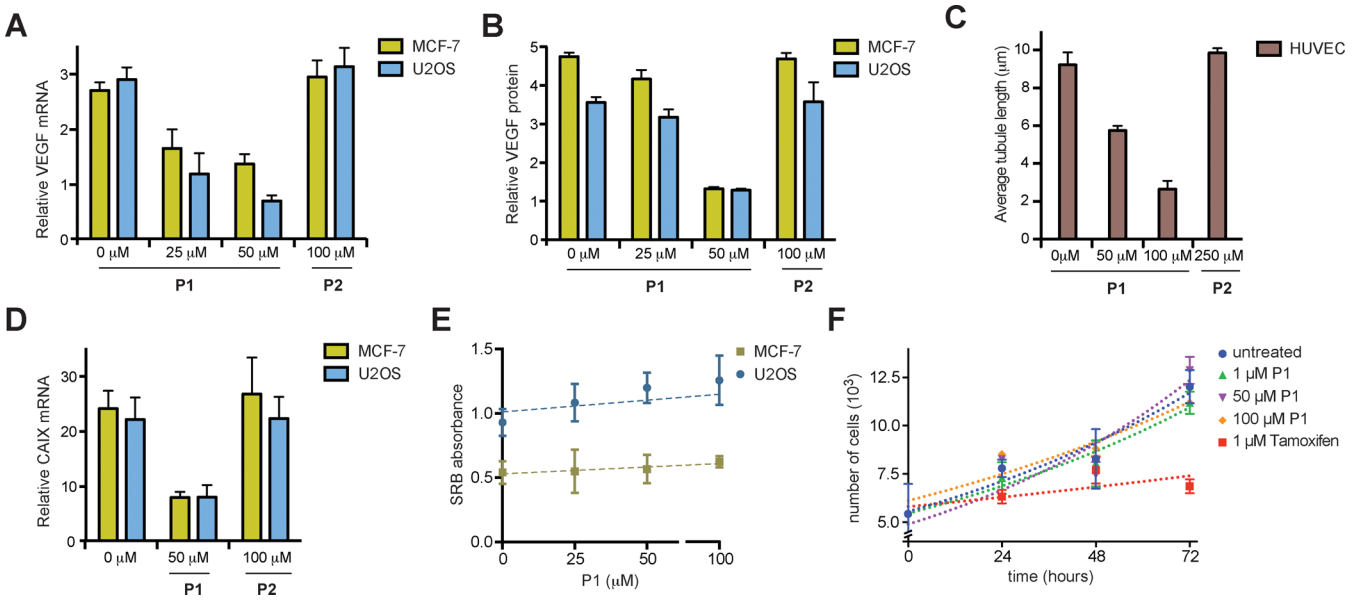

Figure 5. Inhibition of hypoxia response in MCF-7 and U2OS cells by P1. (A) qPCR analysis shows the dose-dependent reduction of VEGF mRNA, elevated by ~3-fold in hypoxia (1 = normoxic levels), by P1 in hypoxic MCF-7 and U2OS cells; 100 μM P2 (control) has no effect in either cell line. (B) VEGF protein level, elevated by 3- to 5-fold in hypoxia (1 = normoxic levels), is also reduced by P1 in hypoxic MCF-7 and U2OS cells; 100 μM P2 (control) has no effect in either cell line. (C) P1 pretreatment causes the dose-dependent reduction of tubule length in hypoxic HUVECs; 250 μM P2 (control) has no effect. For representative images, see Figure S8. (D) qPCR analysis shows 50 μM P1 significantly reduces CAIX mRNA, which is elevated by ~25-fold in hypoxia (1 = normoxic levels); 100 μM P2 (control) has no effect. (E) SRB assay results reveal that 100 μM P1 is not cytotoxic to MCF-7 or U2OS cells. (F) Cell proliferation assays show that 100 μM P1 has no effect on MCF-7 proliferation over 72 h, whereas 1 μM 4-hydroxytamoxifen (control) arrests cell division.

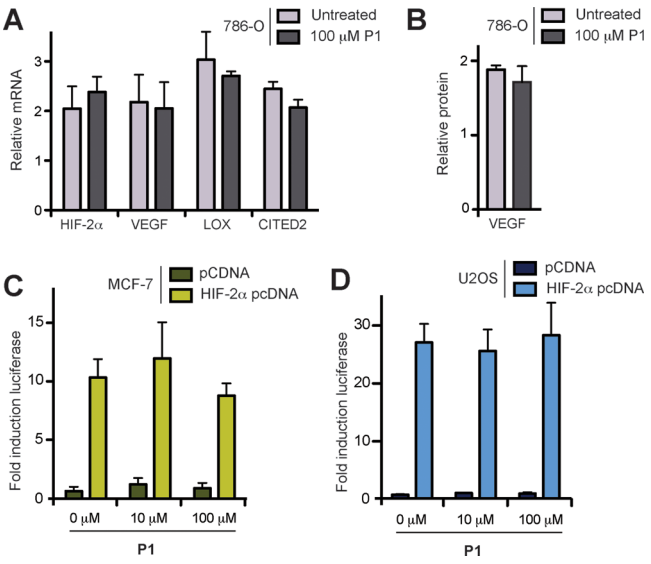

Figure 6. P1 does not affect HIF-2 mediated hypoxia signaling. (A) 100 μM P1 does not affect the transcription of HIF-2α, or HIF-2-promoted VEGF, LOX, CITED2 in hypoxic 786-O cells. (B) 100 μM P1 does not affect VEGF protein levels in hypoxic 786-O cells. (C) P1 does not affect the reporter signal in a HIF-2 luciferase reporter assay in MCF-7 cells. (D) P1 does not affect the reporter signal in a HIF-2 luciferase reporter assay in U2OS cells.

CONCLUSIONS

There is extensive evidence verifying HIF-1 as key in multiple processes critical to cancer progression, and thus a target of significant potential for cancer therapy.[3−5,37] Recent findings such as HIF-1 regulating the survival of tumor cells that escape radiation therapy[38] provides additional evidence for its significance as a target. But the challenges of identifying protein−protein interaction inhibitors in the absence of structural data,[39] combined with the difficulties associated with uncovering transcription factor inhibitors, are substantial. Peptides and macromolecules are increasingly viewed as the optimal scaffold for protein−protein interaction inhibitors,[40] and the high-throughout screening platform employed here has previously proven robust for the identification of cyclic peptide inhibitors of a variety of protein−protein interactions.[24,25,41] When employed for the identification of HIF-1 inhibitors, the platform identified *cyclo*-CLLFVY from a plasmid encoded library of 3.2 million cyclic peptides, via two independent plasmids. Verification of the function of this compound in vitro and in cells revealed that it disrupts HIF-1 dimerization by binding the PAS-B domain of HIF-1α, without affecting HIF-2.

Interestingly, the PAS-B domain of HIF-1α (and HIF-2α) is also targeted by acriflavine.[19] Furthermore, a recently reported heteroaromatic HIF-2 dimerization inhibitor also functions by binding a cavity on HIF-2α PAS-B;[42] although this compound was specifically developed to target HIF-2α PAS-B, the screen for acriflavine and our screen were not biased toward a single domain, yet both identified compounds binding to HIF-α PAS-B. This suggests the PAS-B domain of HIF-α as the optimal point of intervention for a HIF dimerization inhibitor. A homology model of HIF-1α PAS-B mapped onto the NMR structure of HIF-2α PAS-B suggests that the PAS-B cavity is substantially smaller in HIF-1α than HIF-2α.[42] This postulated difference in the cavity size between the two isoforms may be the source of the HIF-1 selectivity observed with *cyclo*-CLLFVY.

As well as its potential for cancer therapy, a specific inhibitor of HIF-1 serves as a chemical tool to verify hypotheses about the unique and sometimes opposing cellular function of HIF-1

dx.doi.org/10.1021/ja402993u | J. Am. Chem. Soc. 2013, 135, 10418−10425

and HIF-2.[2] The compound identified here will also serve to further illuminate the recently reported nontranscriptional function of HIF-1α.[43] A key challenge is the availability of tools to separate the transcriptional function of HIF-1α (or any other transcription factor) from its nontranscriptional function in cells.[41,44] Current approaches that knockdown or knockout the target protein (e.g., siRNA) will not suffice, as they will equally deplete both functions of the protein. In contrast, a HIF-1 dimerization inhibitor only affects the transcriptional function of HIF-1α.

We are currently conducting structural and SAR studies to guide the design of our second-generation HIF-1 dimerization inhibitors. We have previously demonstrated the development of potent, cell-permeable, small molecule protein−protein interaction inhibitors from similarly identified cyclic peptides.[45] The evolution of *cyclo*-CLLFVY, the first example of a molecule that selectively inhibits HIF-1 dimerization in cells, to a small molecule by a similar approach is currently underway in our laboratory.

EXPERIMENTAL SECTION

Oligonucleotides used in this study are detailed in Table S1. DNA synthesis and sequencing was carried out by Eurofins MWG Operon (Germany). All restriction endonucleases were purchased from New England Biolabs; all other molecular biology reagents were purchased from New England Biolabs, Fisher Scientific, or Promega and were used as directed by the manufacturer. Chemical reagents were purchased from Sigma Aldrich, Fisher Scientific, or Merck and were used as received. Amino acids and peptide coupling reagents were obtained from Novabiochem or Matrix Innovations. DNA purification carried out using QIAquick PCR Purification Kit, and plasmid purification was carried out using QIAGEN Plasmid Mini Kit. The CRIM plasmids pAH68 and pAH69 were obtained from the *E. coli* Genetic Stock Centre, Yale University. All peptides were synthesized using a Liberty 1 microwave peptide synthesizer (CEM), and purified on a Waters HPLC system using a Waters C18 Atlantis T3, or a Waters C18 Atlantis Prep OBD column. ITCs were conducted using a MicroCal iTC200 (GE Healthcare). All cell lines were maintained in DMEM (Life Technologies) containing 10% FBS; for aerobic incubation, cells were cultured at 37 °C in 5% CO_2. For hypoxic treatment, cells were cultured and manipulated (DNA, RNA, and protein extraction) in a H35 hypoxia workstation (Don Whitley Scientific) in 1% O_2, 5% CO_2 and 94% N_2. Luminescence was measured in a GloMAX-96 microplate luminometer (Promega). All assays were conducted in triplicate. Data was analyzed in Excel (Microsoft) or Prism (GraphPad Software).

SICLOPPS Screening for HIF-1 Dimerization Inhibitors. The HIF-1 RTHS, associated control RTHS, and SICLOPPS library were constructed as detailed in the Supporting Information. Electrocompetent cells of the HIF-1 RTHS were prepared and transformed with the C+5 SICLOPPS plasmid library. Transformation efficiency, assessed by plating 10-fold serial dilutions of the recovery solution on LB agar supplemented with chloramphenicol (35 μg/mL), was consistently found to be ~5 × 10^7, thus ensuring adequate coverage of the 3.2 × 10^6 member cyclic peptide library. Transformants were washed with minimal media and plated onto minimal media agar plates supplemented with ampicillin (50 μg/mL), spectinomycin (25 μg/mL), kanamycin (50 μg/mL), 3-AT (7.5 μM), IPTG (100 μM), L-arabinose (6.5 μM), and chloramphenicol (35 μg/mL). The plates were incubated for 2−3 days at 37 °C until individual colonies were visible. Colonies were picked and restreaked onto LB agar plates containing ampicillin (50 μg/mL), spectinomycin (25 μg/mL), and chloramphenicol (35 μg/mL) and incubated overnight at 37 °C.

Surviving colonies from these plates were grown overnight and assessed by drop-spotting 10-fold serial dilutions onto minimal media plates, supplemented with antibiotics, IPTG and 3-AT as above, with and without 6.5 μM L-arabinose. Plasmids from strains showing a growth advantage in the presence of arabinose were isolated and retransformed into the original selection strain and reassessed for IPTG-dependent inhibition of growth, and arabinose growth rescue. SICLOPPS plasmids from colonies demonstrating the expected phenotypes were assessed for their HIF-1 specificity by transformation into two identical RTHS, except for the replacement of HIF-1 with unrelated proteins (ATIC, a homodimeric enzyme used in purine biosynthesis, and P6/UEV, a heterodimeric interaction required for the budding of HIV from infected cells).[24,25] Plasmids that caused a growth-advantage in the ATIC or P6/UEV RTHS were discarded for being nonspecific. The activity of the cyclic peptides encoded by the remaining SICLOPPS plasmids was ranked by retransforming into the HIF-1 RTHS and drop spotting of 10-fold dilutions. The identity of the variable insert regions encoding the active cyclic peptides was revealed by DNA sequencing.

Peptide Synthesis. Cyclic peptides were synthesized and characterized as detailed in the Supporting Information.

HIF Luciferase Reporter Assays. Endogenous HIF-1 luciferase reporter assays were conducted as previously reported in U2OS-HRE-luc[15] and MCF-7 cells.[46] For plasmid-expressed HIF-α luciferase reporter assays, MCF-7 and U2OS cells were transiently transfected with plasmids expressing HIF-1α, HIF-2α, or a blank control (pcDNA3.1-HIF-1α, pcDNA3.1-HIF-2α, or pcDNA3.1), a renilla-encoding control (phRL-TK), and a HIF-dependent firefly luciferase reporter construct (pGL2-TK-HRE), using Transfast (Promega) according to the manufacturer's instructions. After 24 h, cells were recovered and plated (4000 cells/well) in 96-well plates (Perkin-Elmer) and incubated for 5 h before either hypoxic or aerobic incubation in presence or absence of cyclic peptide inhibitors. Firefly and renilla activities were determined using Dual-Glo Reagent (Promega) according to the manufacturer's instructions. The luciferase signal was normalized using the corresponding renilla values.

Recombinant Production of HIF-1α and HIF-1β. HIF-1, HIF-2, HIF-1, bHLH, PAS-A, PAS-B, and PAS-B were expressed in *E. coli* (BL21.DE3) as detailed in the Supporting Information.

In Vitro Assays. Pull downs, ELISA, fluorescent binding assays, and ITC were conducted as detailed in the Supporting Information.

Dosing Cells with Inhibitors. Cells were treated with the stated concentrations of inhibitor (P1, P2, or P3) and incubated in normoxia for 4 h, followed by incubation in a hypoxic environment. All manipulation of cell pellets (e.g., lysis, mRNA, and protein extraction) was conducted in a hypoxic environment.

Duolink Proximity Ligation Assay. Duolink proximity ligation assay was conducted using the in situ PLA Kit (O-Link Bioscience, Uppsala, Sweden) according to the manufacturer's instructions. The antibodies used were rabbit monoclonal anti-HIF-1α (NB100-449, Novus Biologicals) and mouse monoclonal anti-HIF-1β (H00000405-B01P, Abnova). Cells were dosed with inhibitors as above and incubated in a hypoxic environment for 4 h, after which they were fixed with cold methanol for 10 min and permeabilized with 0.2% Triton (diluted in PBS) for 10 min. After preincubation with the Duolink Blocking Reagent for 1 h, samples were incubated overnight with the primary antibodies to HIF-1α (1:500) and HIF-1β (1:500). Duolink PLA probes and reagents were added as recommended by the manufacture's instructions.

Quantitative Reverse-Transcription Polymerase Chain Reaction. Total RNA was extracted from MCF-7 and U2OS cells using RNeasy Mini Kit (74104, QIAGEN) and quantified using a Nanodrop ND-1000 spectrophotometer. Complementary DNA was synthesized in a 20 μL reaction containing 1 μg of total RNA, using qScript cDNA SuperMix (95048-100, Quanta Biosciences) according to the manufacturer's instructions. Quantitative real-time PCRs were performed using Universal Taqman PCR master mix (Applied Biosystems) >and the Taqman gene expression assay of interest (Applied Biosystems) on an ABI StepOnePlus Real-Time PCR system (Applied Biosystems). Expression assays used in this study were HIF-1α (00936376_m1), VEGF-A (Hs00173626_m1), CAIX (Hs00154208_m1), LOX (Hs00942480_m1), HIF2α (Hs01026149_m1), CITED2 (Hs01897804_s1), and 18S (Hs99999901_m1). All expression values were normalized using expression of 18S.

Western Immunoblotting. Cells were washed with ice-cold PBS and lysed by incubation on ice in radioimmunoprecipitation assay buffer (50 mM Tris (pH 7.4), 150 μM NaCl, 1 mM EDTA, 1% v/v Triton X-100), and protease inhibitor cocktail (Sigma) for 20 min. Lysates were centrifuged at 14 500 rpm for 15 min at 4 °C, and the protein concentration in the supernatant quantified by Bradford assay. Proteins were separated on precast NuPAGE 4% to 12% polyacrylamide gradient Bis−Tris gels (Invitrogen) under denaturing conditions, transferred to PVDF membranes (Invitrogen), and subjected to immunoblot analysis. Mouse monoclonal anti-HIF-1α (610958, BD Biosciences) and rabbit anti-β-actin (ab8226, Abcam) antibodies were diluted (1:250 and 1:10 000, respectively) in PBS containing 5% nonfat powdered milk and 0.1% Tween-20 and then incubated with the membrane overnight at 4 °C. Horseradish peroxidase conjugated secondary antibodies (Cell Signaling) were used. Bound immunocomplexes were detected using ECL prime Western blot detection reagent (RPN2232, GE Healthcare).

■ ASSOCIATED CONTENT

Supporting Information

Supporting Information includes Figures S1−S9, Tables S1 and S2, and supplemental methods. This material is available free of charge via the Internet at http://pubs.acs.org

■ AUTHOR INFORMATION

Corresponding Author

a.tavassoli@soton.ac.uk

Present Address

[∇]P.A.T.: Institute for Cancer Sciences, University of Manchester, St. Mary's Hospital, Manchester M13 9WL, UK.

Author Contributions

[#]E.M. and I.K.N. contributed equally to this work.

Notes

The authors declare no competing financial interest.

■ ACKNOWLEDGMENTS

We gratefully acknowledge funding of this work by Cancer Research UK (Career Establishment Award A10263 to A.T., and Drug Discovery Grant A9984 to A.T.), the Gerald Kerkut Charitable Trust (Ph.D. studentship for C.E.L. to A.T. and P.A.T.), and the Biotechnology and Biological Sciences Research Council (Doctoral Training Award for I.K.N. to A.T.). We thank Peter Gimeson and GE Healthcare for assistance with ITC, and Prof. Christopher Pugh, Dr. Christopher Bradfield, and Dr. Oliver Hankinson for providing HIF-1β cDNA. We are grateful to Prof. Margaret Ashcroft for U2OS-HRE-luc and U2OS-luc control cells. We also thank Dr. Daniel Asby, Alex Hoose, Dr. David Rusling, Dr. Alison Donlevy, Dr Samantha Larkin, and Dr. Josephine Corsi for helpful discussions and technical assistance.

■ REFERENCES

(1) Wang, G. L.; Jiang, B. H.; Rue, E. A.; Semenza, G. L. *Proc. Natl. Acad. Sci. U.S.A.* **1995**, *92*, 5510.

(2) Keith, B.; Johnson, R. S.; Simon, M. C. *Nat. Rev. Cancer* **2012**, *12*, 9.

(3) Harris, A. L. *Nat. Rev. Cancer* **2002**, *2*, 38.

(4) Semenza, G. L. *Nat. Rev. Cancer* **2003**, *3*, 721.

(5) Giaccia, A.; Siim, B. G.; Johnson, R. S. *Nat. Rev. Drug Discovery* **2003**, *2*, 803.

(6) Bardos, J. I.; Ashcroft, M. *Bioessays* **2004**, *26*, 262.

(7) Jaakkola, P.; Mole, D. R.; Tian, Y. M.; Wilson, M. I.; Gielbert, J.; Gaskell, S. J.; Kriegsheim, A.; Hebestreit, H. F.; Mukherji, M.; Schofield, C. J.; Maxwell, P. H.; Pugh, C. W.; Ratcliffe, P. J. *Science* **2001**, *292*, 468.

(8) Ivan, M.; Kondo, K.; Yang, H.; Kim, W.; Valiando, J.; Ohh, M.; Salic, A.; Asara, J. M.; Lane, W. S.; Kaelin, W. G., Jr. *Science* **2001**, *292*, 464.

(9) Chilov, D.; Camenisch, G.; Kvietikova, I.; Ziegler, U.; Gassmann, M.; Wenger, R. H. *J. Cell Sci.* **1999**, *112* (Pt 8), 1203.

(10) Ebert, B. L.; Bunn, H. F. *Mol. Cell. Biol.* **1998**, *18*, 4089.

(11) Manalo, D. J.; Rowan, A.; Lavoie, T.; Natarajan, L.; Kelly, B. D.; Ye, S. Q.; Garcia, J. G.; Semenza, G. L. *Blood* **2005**, *105*, 659.

(12) Schodel, J.; Oikonomopoulos, S.; Ragoussis, J.; Pugh, C. W.; Ratcliffe, P. J.; Mole, D. R. *Blood* **2011**, *117*, e207.

(13) Jewell, U. R.; Kvietikova, I.; Scheid, A.; Bauer, C.; Wenger, R. H.; Gassmann, M. *FASEB J.* **2001**, *15*, 1312.

(14) Kung, A. L.; Wang, S.; Klco, J. M.; Kaelin, W. G.; Livingston, D. M. *Nat. Med.* **2000**, *6*, 1335.

(15) Chau, N. M.; Rogers, P.; Aherne, W.; Carroll, V.; Collins, I.; McDonald, E.; Workman, P.; Ashcroft, M. *Cancer Res.* **2005**, *65*, 4918.

(16) Escuin, D.; Simons, J. W.; Giannakakou, P. *Cancer Biol. Ther.* **2004**, *3*, 608.

(17) Jones, D. T.; Harris, A. L. *Mol. Cancer Ther.* **2006**, *5*, 2193.

(18) Kung, A. L.; Zabludoff, S. D.; France, D. S.; Freedman, S. J.; Tanner, E. A.; Vieira, A.; Cornell-Kennon, S.; Lee, J.; Wang, B.; Wang, J.; Memmert, K.; Naegeli, H. U.; Petersen, F.; Eck, M. J.; Bair, K. W.; Wood, A. W.; Livingston, D. M. *Cancer Cell* **2004**, *6*, 33.

(19) Lee, K.; Zhang, H.; Qian, D. Z.; Rey, S.; Liu, J. O.; Semenza, G. L. *Proc. Natl. Acad. Sci. U.S.A.* **2009**, *106*, 17910.

(20) Nordgren, I. K.; Tavassoli, A. *Chem Soc Rev* **2011**, *40*, 4307.

(21) Rapisarda, A.; Uranchimeg, B.; Scudiero, D. A.; Selby, M.; Sausville, E. A.; Shoemaker, R. H.; Melillo, G. *Cancer Res.* **2002**, *62*, 4316.

(22) Welsh, S.; Williams, R.; Kirkpatrick, L.; Paine-Murrieta, G.; Powis, G. *Mol. Cancer Ther.* **2004**, *3*, 233.

(23) Horswill, A. R.; Savinov, S. N.; Benkovic, S. J. *Proc. Natl. Acad. Sci. U.S..A* **2004**, *101*, 15591.

(24) Tavassoli, A.; Benkovic, S. J. *Angew. Chem., Int. Ed.* **2005**, *44*, 2760.

(25) Tavassoli, A.; Lu, Q.; Gam, J.; Pan, H.; Benkovic, S. J.; Cohen, S. N. *ACS Chem. Biol.* **2008**, *3*, 757.

(26) Scott, C. P.; Abel-Santos, E.; Wall, M.; Wahnon, D. C.; Benkovic, S. J. *Proc. Natl. Acad. Sci. U.S.A.* **1999**, *96*, 13638.

(27) Tavassoli, A.; Benkovic, S. J. *Nat Protoc* **2007**, *2*, 1126.

(28) Ding, Y.; Xu, M. Q.; Ghosh, I.; Chen, X.; Ferrandon, S.; Lesage, G.; Rao, Z. *J. Biol. Chem.* **2003**, *278*, 39133.

(29) Koslowski, M.; Luxemburger, U.; Tureci, O.; Sahin, U. *Oncogene* **2011**, *30*, 876.

(30) Soderberg, O.; Gullberg, M.; Jarvius, M.; Ridderstrale, K.; Leuchowius, K. J.; Jarvius, J.; Wester, K.; Hydbring, P.; Bahram, F.; Larsson, L. G.; Landegren, U. *Nat. Methods* **2006**, *3*, 995.

(31) Forsythe, J. A.; Jiang, B. H.; Iyer, N. V.; Agani, F.; Leung, S. W.; Koos, R. D.; Semenza, G. L. *Mol. Cell. Biol.* **1996**, *16*, 4604.

(32) Calvani, M.; Rapisarda, A.; Uranchimeg, B.; Shoemaker, R. H.; Melillo, G. *Blood* **2006**, *107*, 2705.

(33) Wykoff, C. C.; Beasley, N. J.; Watson, P. H.; Turner, K. J.; Pastorek, J.; Sibtain, A.; Wilson, G. D.; Turley, H.; Talks, K. L.; Maxwell, P. H.; Pugh, C. W.; Ratcliffe, P. J.; Harris, A. L. *Cancer Res.* **2000**, *60*, 7075.

(34) Skehan, P.; Storeng, R.; Scudiero, D.; Monks, A.; McMahon, J.; Vistica, D.; Warren, J. T.; Bokesch, H.; Kenney, S.; Boyd, M. R. *JNCI, J. Natl. Cancer Inst.* **1990**, *82*, 1107.

(35) Maxwell, P. H.; Wiesener, M. S.; Chang, G. W.; Clifford, S. C.; Vaux, E. C.; Cockman, M. E.; Wykoff, C. C.; Pugh, C. W.; Maher, E. R.; Ratcliffe, P. J. *Nature* **1999**, *399*, 271.

(36) Carroll, V. A.; Ashcroft, M. *Cancer Res.* **2006**, *66*, 6264.

(37) Melillo, G. *Mol. Cancer Res.* **2006**, *4*, 601.

(38) Harada, H.; Inoue, M.; Itasaka, S.; Hirota, K.; Morinibu, A.; Shinomiya, K.; Zeng, L.; Ou, G.; Zhu, Y.; Yoshimura, M.; McKenna, W. G.; Muschel, R. J.; Hiraoka, M. *Nat. Commun.* **2012**, *3*, 783.

(39) Wells, J. A.; McClendon, C. L. *Nature* **2007**, *450*, 1001.

(40) Mullard, A. *Nat. Rev. Drug Discovery* **2012**, *11*, 173.

(41) Birts, C. N.; Nijjar, S. K.; Mardle, C. A.; Hoakwie, F.; Duriez, P. J.; Blaydes, J. P.; Tavassoli, A. *Chem. Sci.* **2013**, *4*, 3046.
(42) Scheuermann, T. H.; Li, Q.; Ma, H. W.; Key, J.; Zhang, L.; Chen, R.; Garcia, J. A.; Naidoo, J.; Longgood, J.; Frantz, D. E.; Tambar, U. K.; Gardner, K. H.; Bruick, R. K. *Nat. Chem. Biol.* **2013**, *9*, 271.
(43) Hubbi, M. E.; Kshitiz; Gilkes, D. M.; Rey, S.; Wong, C. C.; Luo, W.; Kim, D. H.; Dang, C. V.; Levchenko, A.; Semenza, G. L. *Sci. Signaling* **2013**, *6*, ra10.
(44) Huang, L. E. *Science* **2013**, *339*, 1285.
(45) Spurr, I. B.; Birts, C. N.; Cuda, F.; Benkovic, S. J.; Blaydes, J. P.; Tavassoli, A. *ChemBioChem* **2012**, *13*, 1628.
(46) Wang, X. H.; Cavell, B. E.; Syed Alwi, S. S.; Packham, G. *Biochem. Pharmacol.* **2009**, *78*, 261.